

Underlying Event Studies at ATLAS and CDF

D. Kar, for the ATLAS and CDF Collaborations

IKTP, TU Dresden, Dresden, Germany

Abstract.

Improving our understanding and modeling of the underlying event in high energy collider environment is important for more precise measurements at the LHC. CDF Run II data for the underlying event associated with Drell-Yan lepton pair production and early ATLAS data measuring underlying event activity with respect to the leading transverse momentum track are presented. The data are compared with several QCD Monte Carlo models. It is seen that no current standard Monte Carlo tune adequately describes all the early ATLAS data and CDF data simultaneously. The underlying event observables presented here are particularly important for constraining the energy evolution of multiple parton interaction models.

Keywords: Underlying Event, Multiple Parton Interaction, Monte Carlo Tuning

PACS: 12.38.-t, 13.85.-t

INTRODUCTION: THE UNDERLYING EVENT

To perform many precise Standard Model measurements or search for new physics phenomena at hadron colliders, it is essential to have a good understanding not only of the short-distance “hard” scattering process, but also of the accompanying interactions of the rest of the proton – collectively termed the “underlying event” (UE). This includes the beam-beam remnants (BBR) plus the multiple parton interaction (MPI). It is impossible to uniquely separate the underlying event from the hard scattering process on an event-by-event basis. However, observables can be measured which are sensitive to its properties.

This paper reports the measurement of underlying event observables that have been performed in Tevatron $p\bar{p}$ collisions in dijet and Drell-Yan events at the CDF experiment in Run I [1] and Run II [2] at center-of-mass energies of $\sqrt{s} = 1.8$ TeV and 1.96 TeV respectively, and in LHC pp collisions at ATLAS experiment with the leading charged track at $\sqrt{s} = 900$ GeV and 7 TeV [3].

The leading calorimeter jet (reconstructed with the MidPoint algorithm [4] having jet radius $R = 0.7$) in the region $|\eta| < 2$ or Z-bosons decaying into Drell-Yan (DY) lepton pair was taken as the hard scattering process in CDF, with respect to which the underlying event was measured. The charged particles in the range $p_T > 0.5$ GeV and $|\eta| < 1$ were selected. For the DY analysis, only the region of Z-boson, defined as $70 \text{ GeV} < M_{ll} < 110 \text{ GeV}$, was considered. For Drell-Yan lepton pair production, the outgoing lepton anti-lepton pair in the final state means the absence of colored final state radiation. Hence it provides a very clean way to study the underlying event.

The track with the largest p_T in the event – referred to as the “leading” track – is used in ATLAS. The axis given by the the leading track is well-defined for all events, and is highly correlated with the axis of the hard scattering in high p_T events. A single

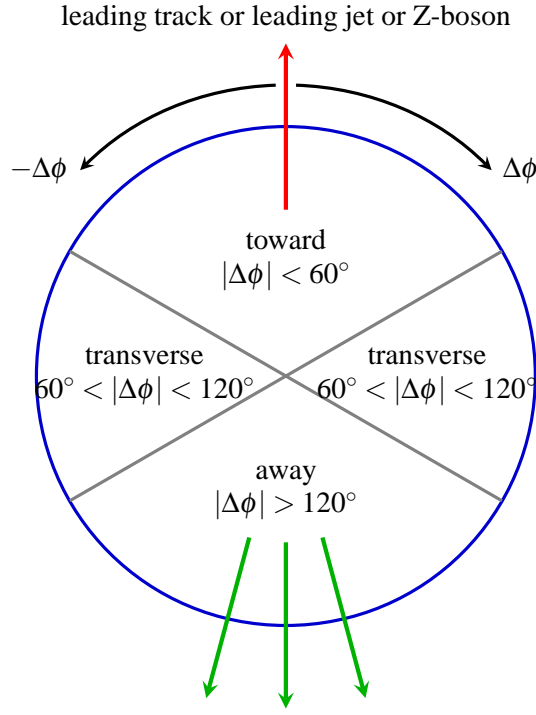


FIGURE 1. Definition of the toward, transverse and away regions in the azimuthal angle with respect to the leading object.

track is used as opposed to a jet or the decay products of a massive gauge boson, as it allows significant results to be derived with limited luminosity and avoids the systematic measurement complexities of alignment with more complex objects. Only events with leading track $p_T > 1$ GeV within the inner detector, $|\eta| < 2.5$, were considered, in order to reject events where the leading track selection can potentially introduce large systematic effects, and also to reduce the contribution from diffractive hard scattering processes. All the other tracks were required to have $p_T > 500$ MeV and the same η range.

As illustrated in Figure 1, the azimuthal angular difference between charged tracks and the leading object, $|\Delta\phi| = |\phi - \phi_{\text{leading object}}|$, is used to define the following three azimuthal regions, for both ATLAS and CDF analysis:

- $|\Delta\phi| < 60^\circ$, the “toward region”;
- $60^\circ < |\Delta\phi| < 120^\circ$, the “transverse region”; and
- $|\Delta\phi| > 120^\circ$, the “away region.”

The transverse regions are most sensitive to the underlying event, since they are generally perpendicular to the axis of hardest scattering and hence have the lowest level of activity from this source. The observables examined in this analysis are corrected back from detector level to particle level, which can be compared directly with the QCD MC models. The detector level corresponds to the tracks passing the corresponding anal-

ysis selection criteria, and the particle level corresponds to distributions with primary charged particles ¹.

The UE may involve contributions from both hard and soft physics, where “soft” labels interactions with low transverse momentum transfer between the scattering particles. Soft interactions cannot reliably be calculated with perturbative QCD, and are generally understood within the context of different phenomenological models, usually implemented in MC event generators. These models contain many parameters whose values are not *a priori* known. Therefore to obtain insight into the nature of soft QCD processes, and to optimize the description of UE backgrounds for studies of hard-process physics, the model parameters must be fitted to experimental data. This tuning effort has been very active in recent years, and the data presented here is an important input for these efforts.

CDF data are compared with PYTHIA [5] tunes A and AW [6] and HERWIG [7]. ATLAS data is compared with predictions by PYTHIA with the ATLAS MC09 [8], DW [9], and Perugia0 [10] tunes, by HERWIG+JIMMY [7, 11] with the ATLAS MC09 tune, and by PHOJET [12].

RESULTS

Charged particle multiplicity

The charged particle multiplicity density from CDF and ATLAS measurements in the transverse region are shown in Figure 2. In Figure 3 the activities in all three regions are compared, and finally in Figure 4, the ATLAS results at $\sqrt{s} = 900$ GeV and 7 TeV are compared.

The average number of charged particles in the transverse region increases with leading p_T , until it reaches an approximately constant “plateau”. Mostly good agreements is observed with PYTHIA tune A and AW predictions for CDF leading jet and Drell-Yan data, although tune A does not have quite enough activity. However, all the pre-LHC MC tunes considered show at least 10–15% lower activity than the ATLAS data in the transverse region plateau. The PYTHIA DW tune is seen to be the closest model to data for the transverse region.

For Drell-Yan data toward and transverse densities are both small and almost equal. The away density is large due to the away side jet to balance the lepton pair p_T . For the leading track analysis, the toward and away regions are dominated by jet-like activity, yielding gradually rising number densities.

The 900 GeV and 7 TeV ATLAS data show the same trend. The underlying event activity is seen to increase by a factor of approximately two between the 900 GeV and 7 TeV data. This is roughly consistent with the rate of increase predicted by MC models tuned to Tevatron data.

¹ Primary charged particles are defined as those with a mean lifetime $\tau \gtrsim 0.3 \times 10^{-10}$ s, either directly produced in pp interactions or in the decay of particles with a shorter lifetime.

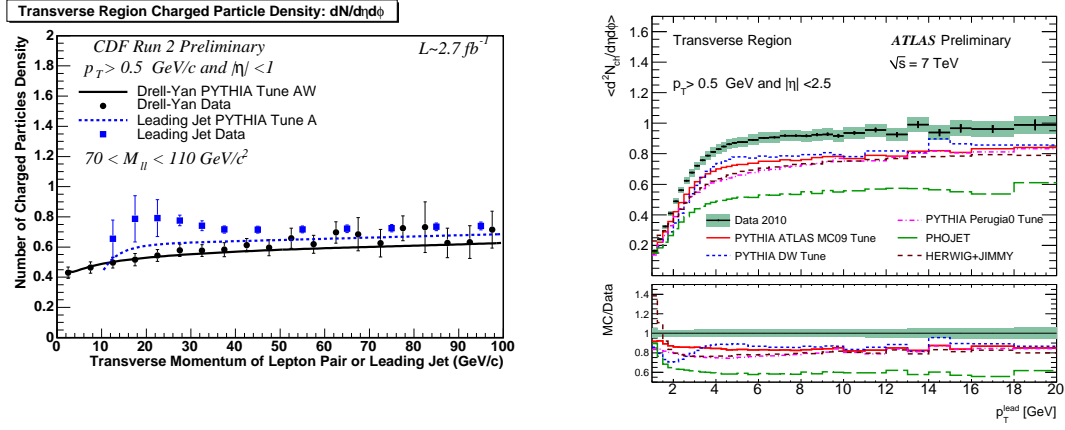


FIGURE 2. CDF data at $\sqrt{s} = 1.96$ TeV (left) and ATLAS data at $\sqrt{s} = 7$ TeV (right), showing the density of the charged particles in the transverse region, compared with different Monte Carlo models.

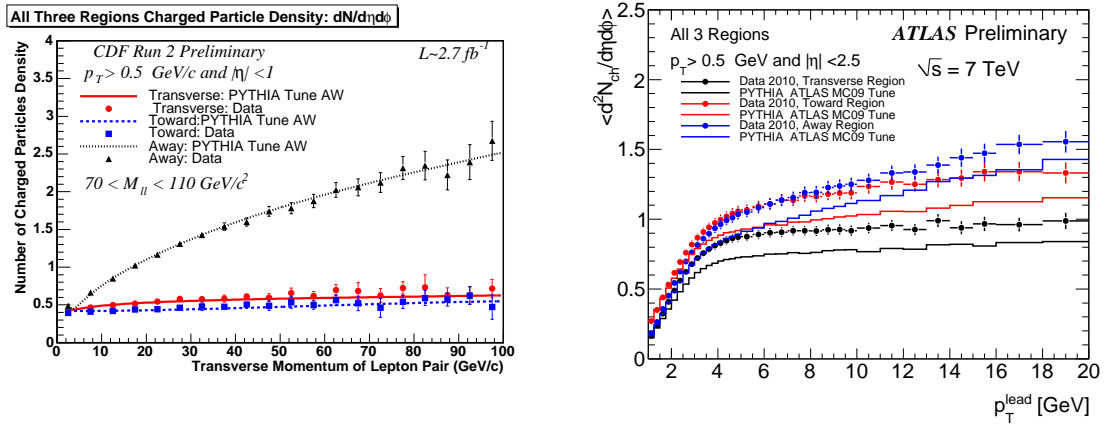


FIGURE 3. CDF Drell-Yan data at $\sqrt{s} = 1.96$ TeV (left) and ATLAS data at $\sqrt{s} = 7$ TeV (right), showing the density of the charged particles in all three regions, compared with different Monte Carlo models.

Charged particle scalar p_T sum

The charged particle scalar p_T sum, $\sum p_T$ density from CDF and ATLAS measurements in the transverse region are shown in Figure 5. In Figure 6 the activities in all three regions are compared.

The summed charged particle p_T in the plateau characterizes the mean contribution of the underlying event to jet energies. Again, we can see that pre-LHC tunes model CDF data better than ATLAS data. The higher number density for ATLAS data implies a higher p_T density as well.

In the ATLAS data, in the toward and away regions, jet-like rising profiles are observed, in contrast to the plateau in the transverse region. The toward region includes

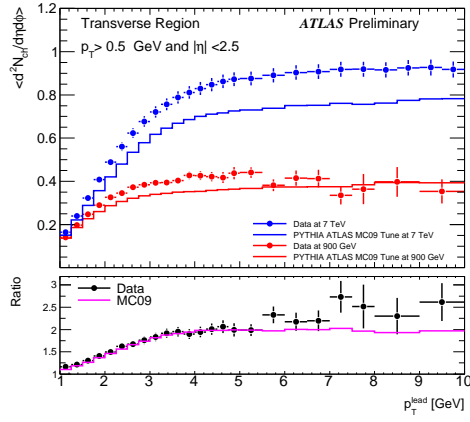


FIGURE 4. Comparison of the ATLAS data at $\sqrt{s}=900$ GeV and $\sqrt{s}=7$ TeV for the density of the charged particles in transverse region, compared with predictions from ATLAS PYTHIA MC09 tune.

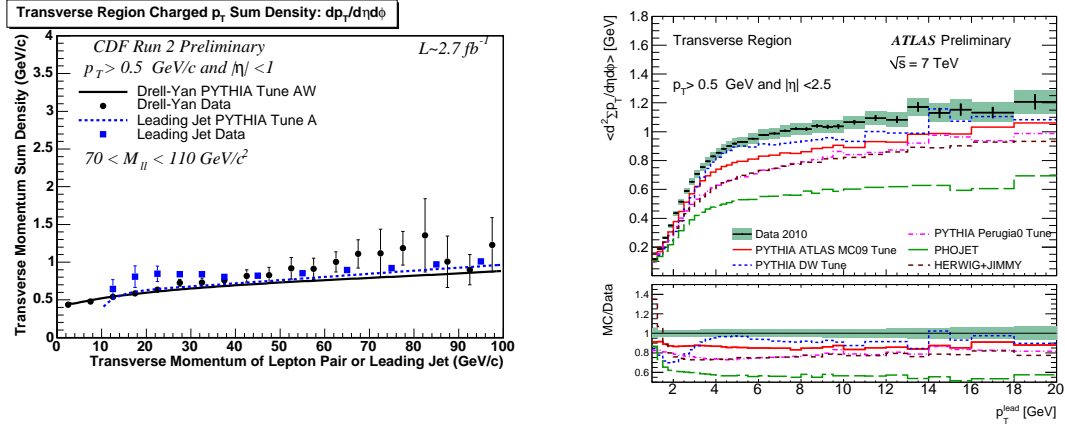


FIGURE 5. CDF data at $\sqrt{s}=1.96$ TeV (left) and ATLAS data at $\sqrt{s}=7$ TeV (right), showing the charged particle scalar p_T sum density in the transverse region, compared with different Monte Carlo models.

the leading charged particle, and has a higher Σp_T than the away region as there is higher probability of high- p_T particles being produced in association with the leading p_T charged particle. In the toward region the highest fraction of energy has been allocated to a single charged particle. This implicitly reduces the number of additional charged particles in that region, since there is less remaining energy to be partitioned. As a result the multiplicity of charged particles is slightly lower in the toward region by comparison to the away region for high p_T^{lead} . The increase of the p_T densities in the toward and away regions indicates the extent of the variation in the charged fraction of the total energy in each region. For the CDF Drell-Yan data, the away density is again large due to the away side jet to balance the lepton pair p_T .

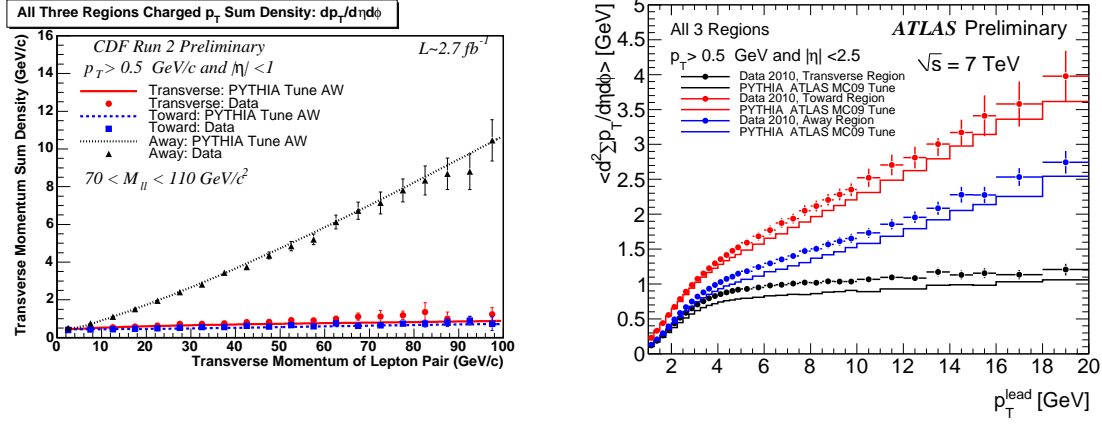


FIGURE 6. CDF Drell-Yan data at $\sqrt{s} = 1.96$ TeV (left) and ATLAS data at $\sqrt{s} = 7$ TeV (right), showing the charged particle scalar p_T sum density in all three regions, compared with different Monte Carlo models.

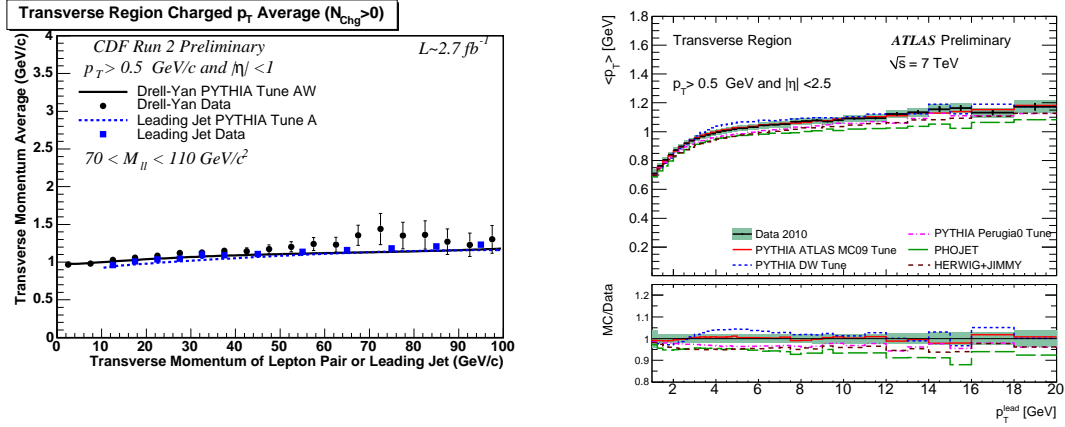


FIGURE 7. CDF data at $\sqrt{s} = 1.96$ TeV (left) and ATLAS data at $\sqrt{s} = 7$ TeV (right), showing the charged particle $\langle p_T \rangle$ in the transverse region, compared with different Monte Carlo models.

Charged particle mean p_T

The charged particle $\langle p_T \rangle$ from CDF and ATLAS measurements in the transverse region are shown in Figure 7. These plots were constructed on an event-by-event basis by dividing the total charged particle p_T in each region by the number of charged particles in that region, requiring at least one charged charged particle in the considered region.

Again, it can be seen that pre-LHC tunes model CDF data better than ATLAS data, but the agreement is better than multiplicity and p_T sum distributions. There is relatively little discrimination between MC models for this observable, all predictions are within $\sim 10\%$ of the data values.

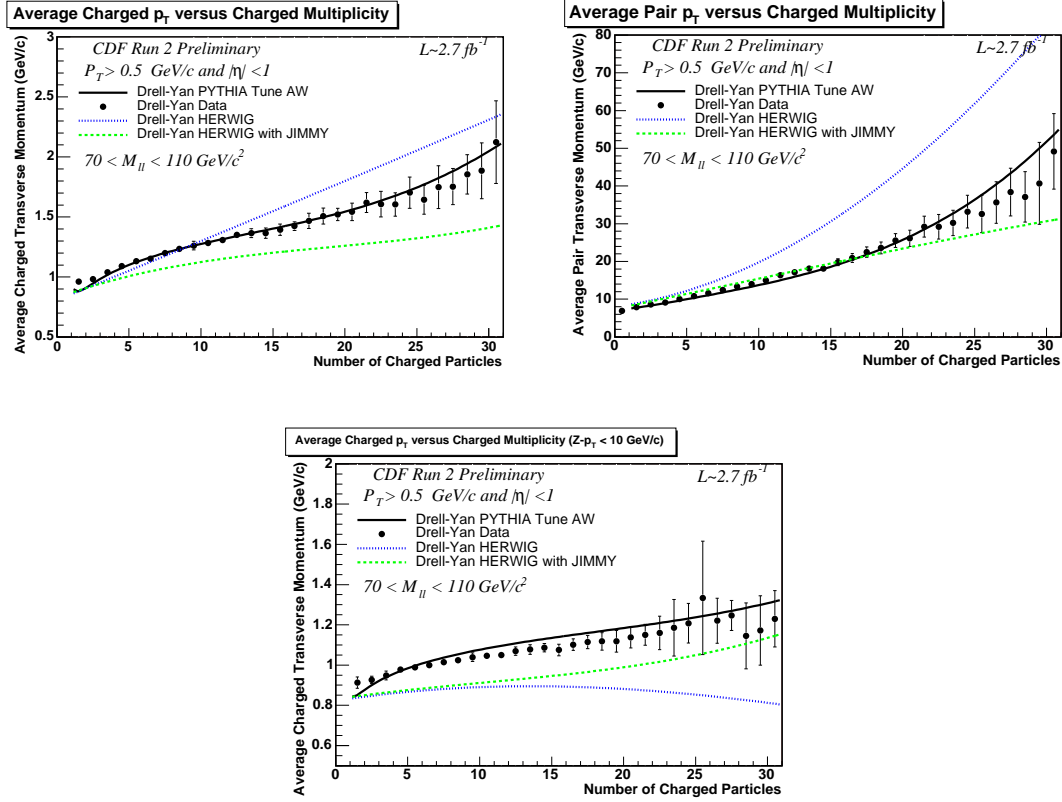


FIGURE 8. CDF Drell-Yan data at $\sqrt{s} = 1.96$ TeV showing the charged particle (top left, and at bottom with restricting $p_T(Z) < 10$ GeV) or the Z-boson (top right) $\langle p_T \rangle$ against the charged particle multiplicity, compared with different Monte Carlo models.

Charged particle mean p_T and multiplicity correlations

The correlation between the mean p_T of charged particles and the charged particle multiplicity in that region is sensitive to the amount of hard (perturbative QCD) versus soft (non-perturbative QCD) processes contributing to the underlying event.

Figure 8 (top left) shows this correlation for CDF Drell-Yan events. HERWIG (without MPI) predicts the $\langle p_T \rangle$ to rise too rapidly as the multiplicity increases, since large multiplicities come from events with a high p_T Z-boson having a large p_T away-side jet. This can be seen clearly in Figure 8 (top right) which shows the average p_T of the Z-boson versus the charged multiplicity. Without MPI the only way of getting large multiplicity is with high $p_T(Z)$ events. For the models with MPI one can get large multiplicity either from high $p_T(Z)$ events or from MPI and hence $\langle p_T(Z) \rangle$ does not rise as sharply with multiplicity like in the data. PYTHIA tune AW describes the Z-boson data fairly well. Figure 8 (bottom) shows the $\langle p_T \rangle$ of charged particles against the multiplicity for charged particles for Z-boson events in which $p_T(Z) < 10$ GeV. We see that $\langle p_T \rangle$ still increases as the multiplicity increases although not as fast. If we require $p_T(Z) <$

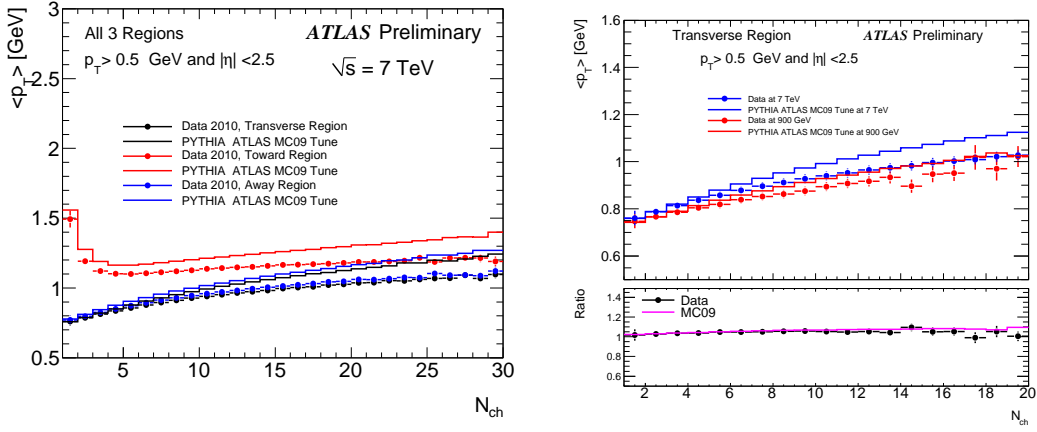


FIGURE 9. ATLAS data at showing the charged particle mean p_T in all three regions at $\sqrt{s} = 7$ TeV (left), and comparison of ATLAS data at $\sqrt{s} = 900$ GeV and $\sqrt{s} = 7$ TeV in transverse region (right).

10 GeV, than HERWIG (without MPI) predicts that the $\langle p_T \rangle$ decreases slightly as the multiplicity increases. This is because without MPI and without the high p_T away-side jet which is suppressed by requiring low p_T (Z), large multiplicities come from events with a lot of initial-state radiation and the particles coming from initial-state radiation are soft. PYTHIA tune AW describes the behavior of $\langle p_T \rangle$ versus the multiplicity fairly well even when we select p_T (Z) < 10 GeV. This strongly suggests that MPI are playing an important role in both these processes.

In Figure 9, the ATLAS profiles in the transverse and away regions are very similar, showing a monotonic increase of $\langle p_T \rangle$ with N_{ch} . The profile of the toward region is different, as it is essentially determined by the requirement of a track with $p_T > 1$ GeV. For $N_{ch} = 1$, it contains only the leading charged particle and as the N_{ch} is increased by inclusion of soft charged particles the average is reduced. However, for $N_{ch} > 5$ jet-like structure begins to form, and the weak rise of the mean p_T is observed. Comparing the 900 GeV and 7 TeV data, it is seen that the mean charged particle p_T vs. N_{ch} profiles are largely independent of the energy scale of the collisions.

Angular distributions

The angular distributions with respect to the leading charged particle of the charged particle number and $\sum p_T$ densities at the center-of-mass energy of 7 TeV at ATLAS, with charged particle $p_T > 0.5$ GeV, are plotted in Figure 10. The leading charged particle taken to be at $\Delta\phi = 0$ has been excluded from the distributions. The data are shown for four different lower cut values in leading charged particle p_T . These distributions are constructed by reflecting $|\Delta\phi|$ about zero, i.e. the region $-\pi \leq \Delta\phi < 0$ is an exact mirror image of the measured $|\Delta\phi|$ region shown in $0 \leq \Delta\phi \leq \pi$.

These distributions show a significant difference in shape between data and MC predictions. With the increase of the leading charged particle p_T , the development of jet-

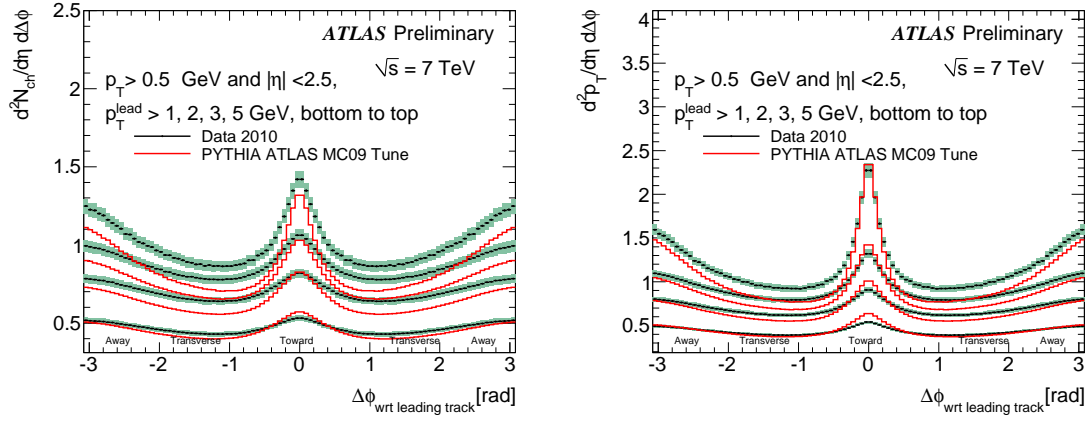


FIGURE 10. ATLAS data showing the ϕ distribution of charged particle multiplicity (left) and scalar Σp_T density (right), with respect to the leading charged particle rotated to $\phi_{\text{leading}} = 0$, excluding the leading charged particle and compared to different MC model predictions. The distributions obtained by restricting the minimum leading charged particle p_T to different values are shown separately. The plots were symmetrized by reflecting them about $\Delta\phi = 0$.

like structure can be observed, and the corresponding sharper rise in transverse regions compared to the MC. MC models essentially predict a stronger correlation than is seen in the data, and this discrepancy in toward region associated particle density was also observed at CDF [13].

SUMMARY AND CONCLUSIONS

One of the goals of these analyses is to provide data that can be used to test and improve MC models for current and future physics studies at the LHC. The underlying event observables presented here are particularly important for constraining the energy evolution of multiple partonic interaction models, since the plateau heights of the underlying event profiles are highly correlated to multiple parton interaction activity. The data at 7 TeV are crucial for MC tuning, since measurements are needed with at least two energies to constrain the energy evolution of MPI activity.

PYTHIA tune A and tune AW do a good job in describing the CDF data on the underlying-event observables for leading jet and Drell-Yan events, respectively, although the agreement between predictions and data is not perfect. The leading-jet data show slightly more activity in the underlying event than PYTHIA Tune A, although they are very similar - which may indicate the universality of underlying event modeling. However, all pre-LHC MC models predict less activity in the transverse region (i.e. in the underlying event) than is actually observed in ATLAS leading track data, for both center-of-mass energies.

There is therefore no current standard MC tune which adequately describes all the early ATLAS data. However, using diffraction-limited minimum bias distributions and the plateau of the underlying event distributions presented here, ATLAS has devel-

oped a new PYTHIA tune AMBT1 (ATLAS Minimum Bias Tune 1) and a new HERWIG+JIMMY tune AUET1 (ATLAS Underlying Event Tune 1) which model the p_T and charged multiplicity spectra significantly better than the pre-LHC tunes of those generators [14, 15]. It is critical to have sensible underlying event models containing our best physical knowledge and intuition, tuned to all relevant available data.

REFERENCES

1. The CDF Collaboration, *Phys. Rev. D* **70**, 072002 (2004).
2. The CDF Collaboration, *Phys. Rev. D* **82**, 034001 (2010).
3. The ATLAS Collaboration, Tech. Rep. ATLAS-CONF-2010-081 (2010), URL <http://cdsweb.cern.ch/record/1298845>.
4. The CDF Collaboration, *Phys. Rev. D* **73**, 052006 (2008).
5. T. Sjostrand, S. Mrenna, and P. Skands, *JHEP* **05**, 026 (2006), hep-ph/0603175.
6. R. Field, and R. C. Group (2005), hep-ph/0510198.
7. G. Corcella, et al. (2002), hep-ph/0210213.
8. The ATLAS Collaboration, Tech. Rep. ATLAS-PHYS-PUB-2010-002 (2010), URL <http://cdsweb.cern.ch/record/1247375>.
9. R. Field, Min-Bias and the Underlying Event at the Tevatron and the LHC, A talk presented at the FERMILAB MC Tuning Workshop, FERMILAB (2002).
10. P. Skands, The Perugia Tunes (2009), arXiv:0905.3418v1.
11. J. M. Butterworth, J. R. Forshaw, and M. H. Seymour, *Z. Phys.* **C72**, 637–646 (1996), hep-ph/9601371.
12. R. Engel, *Z. Phys.* **C66**, 203–214 (1995).
13. R. Field, Early QCD Measurements at the LHC, A talk presented at LHC@BNL: Joint Theory/Experiment Workshop on Early Physics at the LHC, BNL (2010).
14. The ATLAS Collaboration, Tech. Rep. ATLAS-CONF-2010-031 (2010), URL <http://cdsweb.cern.ch/record/1277665>.
15. The ATLAS Collaboration, Tech. Rep. ATLAS-PHYS-PUB-2010-014 (2010), URL <http://cdsweb.cern.ch/record/1303025>.